

See discussions, stats, and author profiles for this publication at: <https://www.researchgate.net/publication/49726788>

Identification of arylamine N-acetyltransferase inhibitors as an approach towards novel anti-tuberculars

ARTICLE *in* PROTEIN & CELL · JANUARY 2010

Impact Factor: 3.25 · DOI: 10.1007/s13238-010-0006-1 · Source: PubMed

CITATIONS

24

READS

85

13 AUTHORS, INCLUDING:



Sanjib Bhakta

Birkbeck, University of London

65 PUBLICATIONS 833 CITATIONS

SEE PROFILE



Elizabeth Fullam

The University of Warwick

27 PUBLICATIONS 658 CITATIONS

SEE PROFILE



Richard Vickers

University of Oxford

28 PUBLICATIONS 373 CITATIONS

SEE PROFILE



Edith Sim

University of Oxford

232 PUBLICATIONS 7,259 CITATIONS

SEE PROFILE

RESEARCH ARTICLE

Identification of arylamine *N*-acetyltransferase inhibitors as an approach towards novel anti-tuberculars

Isaac M. Westwood^{1,2,5*}, Sanjib Bhakta^{1,6*}, Angela J. Russell^{1,2*}, Elizabeth Fullam^{1,2}, Matthew C. Anderton¹, Akane Kawamura^{1,2}, Andrew W. Mulvaney², Richard J. Vickers², Veemal Bhowruth³, Gurdial S. Besra³, Ajit Lalvani⁴, Stephen G. Davies², Edith Sim¹ (✉)

¹ Department of Pharmacology, University of Oxford, Oxford OX1 3QT, United Kingdom

² Chemistry Research Laboratory, Department of Organic Chemistry, University of Oxford, Oxford OX1 3QL, United Kingdom

³ School of Biosciences, University of Birmingham, Edgbaston, Birmingham B15 2TT, United Kingdom

⁴ Tuberculosis Immunology Group, Department of Respiratory Medicine, National Heart and Lung Institute, Wright Fleming Institute of Infection and Immunity, Imperial College London, Norfolk Place, London W2 1PG, United Kingdom

⁵ Current address: Structure-Based Drug Design Team, Sections of Structural Biology and Cancer Therapeutics, Institute of Cancer Research, Chester Beatty Laboratories, London SW3 6JB, United Kingdom

⁶ Current address: Institute of Structural and Molecular Biology, Department of Biological Science, Birkbeck, University of London, London WC1E 7HX, United Kingdom

✉ Correspondence: edith.sim@pharm.ox.ac.uk

Received October 8, 2009; accepted November 3, 2009

ABSTRACT

New anti-tubercular drugs and drug targets are urgently needed to reduce the time for treatment and also to identify agents that will be effective against *Mycobacterium tuberculosis* persisting intracellularly. Mycobacteria have a unique cell wall. Deletion of the gene for arylamine *N*-acetyltransferase (NAT) decreases mycobacterial cell wall lipids, particularly the distinctive mycolates, and also increases antibiotic susceptibility and killing within macrophage of *Mycobacterium bovis* BCG. The *nat* gene and its associated gene cluster are almost identical in sequence in *M. bovis* BCG and *M. tuberculosis*. The gene cluster is essential for intracellular survival of mycobacteria. We have therefore used pure NAT protein for high-throughput screening to identify several classes of small molecules that inhibit NAT activity. Here, we

characterize one class of such molecules—triazoles—in relation to its effects on the target enzyme and on both *M. bovis* BCG and *M. tuberculosis*. The most potent triazole mimics the effects of deletion of the *nat* gene on growth, lipid disruption and intracellular survival. We also present the structure-activity relationship between NAT inhibition and effects on mycobacterial growth, and use ligand-protein analysis to give further insight into the structure-activity relationships. We conclude that screening a chemical library with NAT protein yields compounds that have high potential as anti-tubercular agents and that the inhibitors will allow further exploration of the biochemical pathway in which NAT is involved.

KEYWORDS *N*-acetyltransferase, *Mycobacterium tuberculosis*, triazoles, screening

*These authors contributed equally to the work.

INTRODUCTION

There is an urgent need for new drugs for tuberculosis (TB), and new compounds have been described despite the fact that the targets are not clearly established (Al-Balas et al., 2009). Discovery of new targets is important to identify novel drugs (Cole and Azari, 2005; Makarov et al., 2009). It has been recognized that understanding important metabolic pathways is likely to be a useful route towards new therapies (www.tballiance.org) as a result of the success with an ATPase inhibitor (Diacon et al., 2009). Recent identification of menaquinone biosynthesis as a useful target pathway provides a growing portfolio of potential novel anti-tuberculars (Dhiman et al., 2009). The need for a wide range of candidate targets and molecular classes is insurance for the future (Maxmen and Barry, 2009; Lin et al., 2009). The biggest difficulty with anti-tubercular and indeed anti-microbiological agents is the development of resistance. The development of multi-therapies that work in a short time period is an important aim in order to understand more about the organism that causes tuberculosis and also to overcome the disease. Tuberculosis is a global problem compounded by the emergence of drug-resistant tuberculosis particularly in association with AIDS (Dye, 2006). Whilst tuberculosis is endemic in many developing countries, there are also urban areas in the United Kingdom where TB is now a common disease through the combination of high population density and immigration from countries with endemic TB (Story et al., 2006). *Mycobacterium tuberculosis*, the organism that causes TB, survives within macrophage in the host and is likely to be a contributory factor in the extended duration of therapy required for eradication of tuberculosis, as is the existence of persisting, but non-dividing organisms both in and remote from the human lung (Neyrolles et al., 2006).

Functional genomics has identified possible roles for several previously unknown gene products in *M. tuberculosis* (Rengarajan et al., 2005), and investigation of the role of candidate gene products has also resulted in novel functional information. Arylamine *N*-acetyltransferase (NAT) was initially identified as an interesting target in mycobacterial research because in humans one of the NAT isoenzymes (known as human NAT2) (Boukouvala and Fakis, 2005) had been demonstrated to be responsible for the acetylation and inactivation of the still widely used anti-tubercular drug isoniazid (INH) (Evans et al., 1960; Weber and Hein, 1985). The discovery of a *nat* homolog in *M. tuberculosis* led to the hypothesis that NAT had a role in drug resistance (Payton et al., 1999). The *nat* gene is transcribed and the NAT enzyme is active in both *M. bovis* BCG and *M. tuberculosis* (Upton et al., 2001). To investigate drug resistance, a deletion of the *nat* gene in *M. bovis* BCG was characterized (Bhakta et al., 2004). The major target of isoniazid, a pro-drug which is activated inside mycobacteria, has been the subject of dispute, and it is likely that isoniazid has several targets

(Raman et al., 2005). With isoniazid acetylation by NAT competing with activation of the pro-drug by the *katG* gene product (Nagy et al., 1997; Bhakta et al., 2004), NAT is likely to be a minor target of isoniazid because deleting the *nat* gene resulted in a small increase in the sensitivity of the Δnat strain to isoniazid. However, the effect of knocking out the gene was much more dramatic. The effects on the growth, morphology, lipid composition, sensitivity to antibiotics and most importantly the intracellular killing of the Δnat strain of *M. bovis* BCG within macrophage suggested that the NAT enzyme, *per se*, would be a useful target for anti-tubercular therapy (Bhakta et al., 2004). Deletion of the *nat* gene was the cause of the changes in the genetically modified strain, since complementation of the Δnat strain restored the original phenotype. The observation that the *nat* gene appears to be essential for survival of *M. bovis* BCG within macrophage (Bhakta et al., 2004) is consistent with the observation that the *nat* gene encodes for a protein that is involved in the synthesis of cell wall complex lipids, including mycolates (Bhakta et al., 2004). It has been shown that the *nat* gene is encoded as the last gene within an operon (Anderton et al., 2006). The flanking regions differ by only a single base (in the first gene of the operon) between *M. bovis* BCG and *M. tuberculosis* (Fig. 1). The first two genes of the operon, *HsaA* and *HsaD*, have been identified as essential genes for survival of *M. tuberculosis* within macrophage (Rengarajan et al., 2005). In addition, inhibitors of the HsaC enzyme encoded by the operon (Fig. 1) have a similar effect on the lipid profile as does deletion of the *nat* gene in *M. bovis* BCG, that is the mycolates and complex lipids are diminished but the phospholipids are not (Anderton et al., 2006). More recently, it has become clear that *HsaC* is essential for survival of *M. tuberculosis* in the host (Yam et al., 2009). It has been demonstrated that the operon is part of the KstR regulon that is essential for intracellular survival inside macrophage (Kendall et al., 2007). The genes encoding HsaA–D have a role in cholesterol catabolism (Van der Geize et al., 2008) and the utilization of propionyl CoA as a cofactor by the TBNAT enzyme links the NAT gene product functionally with the operon (Lack et al., 2009).

To obtain more information on the role of the NAT enzyme as a target for anti-tubercular therapy, a high-throughput screen has been established using recombinant NAT protein (Brooke et al., 2003a, b; Russell et al., 2009). The pure recombinant NAT enzyme from *M. tuberculosis* is relatively insoluble with maximum yields approaching approximately 2 mg per Liter of culture (Upton et al., 2001; Sikora et al., 2008; Lack et al., 2009; Fullam et al., 2009). In order to optimize the screening procedure, we have therefore used NAT proteins that have similar substrate specificities but are produced more abundantly as recombinant proteins at around 20 mg per liter of culture and that store well when pure (Westwood et al., 2005; Fullam et al., 2007, 2009). NAT isoenzymes have been characterized from a range of organisms and crystal structures have been obtained for the enzyme from

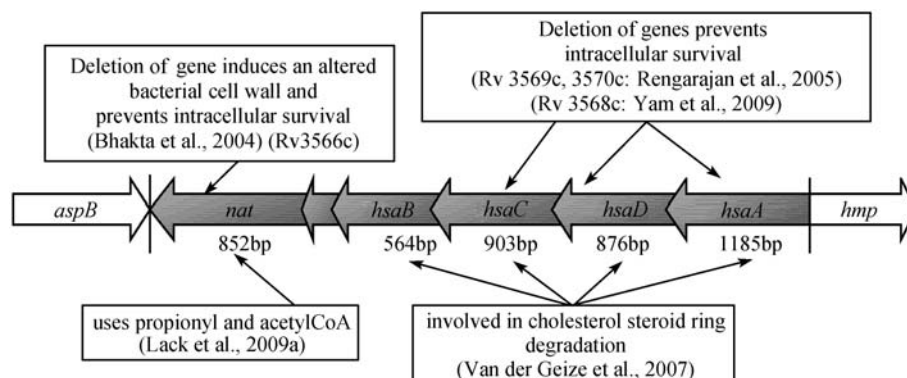


Figure 1. The 'nat' operon in *Mycobacterium tuberculosis* and *Mycobacterium bovis* BCG. The genome sequences of *M. tuberculosis* H₃₇Rv and *M. bovis* BCG are identical in the region shown, except for one nucleotide change in the putative oxidoreductase gene (*HsaA*) (Sim et al., 2008). This nucleotide change leads to an aspartic acid residue in *M. bovis* BCG where the corresponding amino acid in *M. tuberculosis* H₃₇Rv is an asparagine (Sim et al., 2008). The accession numbers for the genes, ordered from *hsaA* to *hsaB*, for *M. tuberculosis* H₃₇Rv are: Rv3570c, Rv3569c, Rv3568c and Rv3567c. Rv3570c and Rv3569c have been shown to be essential for survival inside macrophage (Rengarajan et al., 2005) and *in vivo* (Yam et al., 2009). The corresponding genes in *M. bovis* BCG have the following accession numbers: Mb3601c, Mb3600c, Mb3599c and Mb3598c. The *nat* gene (Rv3566c, Mb3596c), which has also been shown to be required for survival inside macrophage (Bhakta et al., 2004), is preceded by a gene encoding for a hypothetical protein (Rv3566a, Mb3597c).

Salmonella typhimurium (Sinclair et al., 2000), *Pseudomonas aeruginosa* (Westwood et al., 2005), the mycobacterial species *Mycobacterium smegmatis* (Sandy et al., 2002) and more recently from *Mycobacterium marinum* (Fullam et al., 2007; PDB code 2vfb), which is 74% identical to the enzyme from *M. tuberculosis* (Fullam et al., 2009). A preliminary manual screen of a limited range of compounds using the NAT enzyme from *M. smegmatis* had already proved successful in identifying NAT inhibitors (Brooke et al., 2003b). We report here that specific NAT inhibitors mimic the effects of deleting the *nat* gene in *M. bovis* BCG and that these compounds are also effective in inhibiting the growth of *M. tuberculosis*.

RESULTS

Screen design

The substrate specificity profiles of NAT enzymes from a range of bacterial NATs are extremely similar to each other but are distinct from the NAT isoenzymes from humans and other mammals (Westwood et al., 2005; Westwood et al., 2006; Kawamura et al., 2005, 2008). In order to identify compounds that would be unlikely to be metabolized by the human NAT isoenzymes, NAT inhibitors that would be effective against the prokaryotic NAT enzymes but were not inhibitors of the eukaryotic NAT enzymes were sought. NAT enzymes were chosen where sufficient stable recombinant enzyme (tens of milligrams of each protein) was available. The eukaryotic enzymes were pure hamster NAT2 (shNAT2) and its human homolog human NAT1 (hNAT1) (Kawamura et al., 2005; Wang et al., 2005). The prokaryotic NAT enzymes were from *M. smegmatis* (Sandy et al., 2002) (MSNAT), *S.*

typhimurium (Sinclair et al., 2000) (STNAT) and *P. aeruginosa* (Westwood et al., 2005) (PANAT). The NAT inhibitor screening method is as described previously (Brooke et al., 2003a, b; Russell et al., 2009). The assay method relies on a colorimetric reaction linked to the NAT-catalysed hydrolysis of acetyl Coenzyme A (acetylCoA), which occurs at a greatly enhanced rate in the presence of a substrate for the acetylation reaction. Conditions for a linear initial rate of acetylCoA hydrolysis were determined for each NAT enzyme included in the screen. Recombinant NAT from *M. marinum* (MMNAT) was also used for quantitative analyses of compounds as specific prokaryotic NAT inhibitors following the screening process, and a crystal structure for the *M. marinum* enzyme is also now available (Fullam et al., 2007).

Inhibition of the hydrolysis of acetylCoA was determined using a library of 5000 drug-like compounds (Russell et al., 2009). The compounds in the library had been compiled to represent a structurally diverse set of chemically tractable entities without reactive groups such as aldehydes, Schiff bases or aminals, or known cytotoxic agents (such as polynitro aromatics). The structures are also amenable to both resynthesis and rapid diversification (Russell et al., 2009). Each compound was screened in triplicate against each enzyme with two substrates. Hits in the screen were compounds that inhibited, with both substrates, at least two of the prokaryotic NAT enzymes more than 50% at 30 μ M and that did not inhibit either of the eukaryotic NAT enzymes more than 20% at the same concentration. This was also coupled with Z-score analysis to compensate for any systematic errors related to plate position (Brooke et al., 2003a). The strategy used was designed to maximize the hit rate and to minimize both false-positive and false-negative results.

Using this screening strategy, a number of structurally distinct small molecules were identified as hits. The sultam inhibitors, which were identified in the previous one-enzyme screen (Brooke et al., 2003b), did not appear as hits in this more discriminating five-enzyme screen. In order to confirm the inhibitory activity, the hits were re-screened using more stringent criteria against the same panel of five NAT enzymes. Only compounds that satisfied the criteria of showing over 80% inhibition of at least two prokaryotic enzymes and showing less than 20% inhibition of the eukaryotic enzymes at 30 μ M in the re-screen were carried forward (Fig. 2). At the completion of the second round of screening, of the six compounds that were identified in distinct chemical classes, two compounds were weak NAT inhibitors upon retesting with the *M. marinum* NAT enzyme such that less than 80% inhibition was found at 30 μ M. Neither of these compounds was therefore pursued further.

For the compounds that were investigated further, effects on growth of *M. tuberculosis* H37Rv and *M. bovis* BCG on agar have been determined (Anderton et al., 2006). Table 1 shows data for the remaining four compounds: compound 1 inhibits PANAT at less than 10 μ M but is less effective against the *M. marinum* enzyme. It is not a good inhibitor of growth of *M. tuberculosis* and therefore this compound was not pursued further. Of the three remaining compounds, pyrazole 2 had an IC_{50} of 18.5 ± 1.0 μ M against *M. marinum* NAT and had an MIC of less than 10 μ g/mL against both *M. bovis* BCG and *M. tuberculosis* (Table 1). In addition, compound 3 was observed to inhibit MMNAT with an IC_{50} of 6.0 ± 1.0 μ M and to inhibit the growth of *M. bovis* BCG and *M. tuberculosis* with a minimum inhibitory concentration (MIC) of less than 5 μ g/mL. Compound 3 had previously tested positive as an anti-tubercular

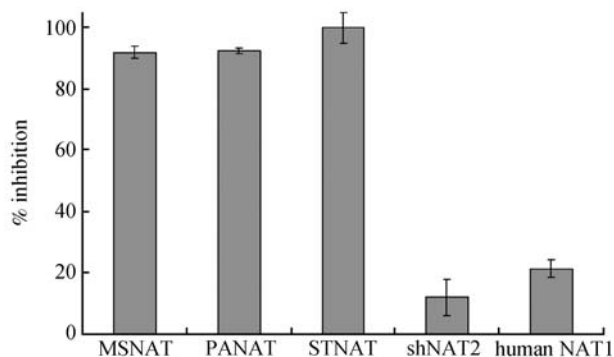


Figure 2. Specificity of screen for prokaryotic NAT enzymes. Compound 3 (Table 1) was tested at 30 μ M against five NAT enzymes from *M. smegmatis* (MSNAT), *S. typhimurium* (STNAT), *Pseudomonas aeruginosa* (PANAT) and also against two eukaryotic enzymes, hamster NAT2 (shNAT2) and human NAT1. In each case pure recombinant enzyme was tested and the results are shown as the mean \pm SD of triplicate determinations of percentage inhibition of hydrolysis of acetylCoA in the presence of arylamine substrate as described in Materials and Methods.

agent in an extensive survey of 240 compounds, but no mechanistic information was provided (Jeney et al., 1956). Compound 4, a 1,2,4 triazole-3-thione derivative, was shown on resynthesis to have an IC_{50} of 6.4 μ M with PANAT and around 10 μ M with MMNAT and to inhibit growth of *M. tuberculosis* with an MIC of less than 10 μ g/mL. We have concentrated on compounds 3 and 4. Since compound 3 has a chiral centre, the present study describes the analysis of compound 4 and its analogues on NAT and *M. tuberculosis*. Structures incorporating the 1,2,4-triazole-3-thione motif and related examples (Macaev et al., 2005; Foroumadi et al., 2006) have been reported recently to have anti-tubercular activity although no mechanism of action has been proposed.

To summarize, a series of compounds that inhibit bacterial NAT were shown to suppress growth of *M. tuberculosis* at 10 μ g/mL or lower concentration, and we report here on a detailed analysis of the 1,2,4-triazole-3-thione derivative (compound 4).

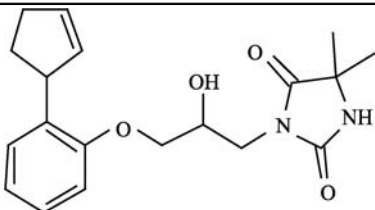
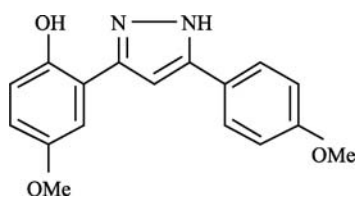
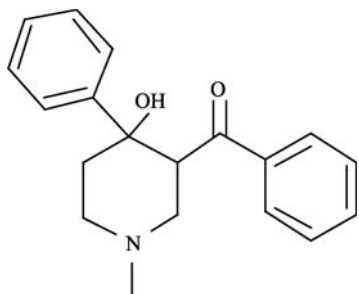
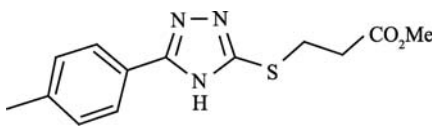
Compound 4 and its structural analogues

All of the compounds shown in Table 1 were resynthesised to confirm their identity, but we focus here on the resynthesis of compound 4 and a series of analogues. Compound 4 was synthesised as follows: *p*-tolyl chloride was condensed with thiosemicarbazide in pyridine (Kane et al., 1994; Singh, 1996). Cyclisation of the condensation product was effected by subsequent treatment with 1 M aqueous sodium bicarbonate to produce the precursor 5-(4'-methylphenyl)-1,2,4-triazole-3-thione (5) in 62% yield and 97% purity over two steps. Alkylation of 5 with methyl 3-bromopropionate produced the target methyl ester (4) in 52% isolated yield (Scheme 1).

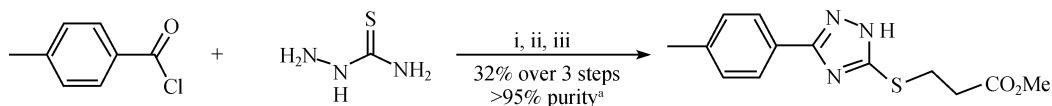
Methyl ester 4 was subjected to saponification with lithium hydroxide. The free acid formed (6) was found to be a weaker inhibitor of NAT activity than 4 (IC_{50} value of 20.1 ± 0.9 μ M), and showed no inhibition of the growth of *M. bovis* BCG *in vitro* at any of the concentrations tested (up to 100 μ g/mL).

The substituents at both the 3-position and the 5-position of the 1,2,4-triazole ring of 4 were varied to allow preliminary investigations into the structure-activity relationships. Consequently, a range of 1,2,4-triazole-3-thiones (7–12) was synthesised from their corresponding acid chlorides. With the exception of compound 7, the purified yields varied between 44% and 98% (Table 2). The purity of all synthesised compounds was >95%, as assessed by HPLC (described in Materials and Methods). The 1,2,4-triazole-3-thiones were then treated with a range of electrophiles to generate an array of compounds with a range of substituents on the 3-position of the 1,2,4-triazole ring. An excess of the electrophile was used in order to drive the reaction to completion. Unreacted electrophile was subsequently removed by adding a nucleophilic scavenger resin, in order to avoid the need for further purification steps (Ley, 2000). Therefore, treatment of the crude reaction mixtures with polymer-supported

Table 1 Structural classes of NAT inhibitors identified through high-throughput screening

ID	structure	IC ₅₀ against PANAT (μ M)	IC ₅₀ against MMNAT (μ M)	MIC against <i>M. tuberculosis</i> (μ g/mL)
1		17.7 \pm 1.5	33.0 \pm 1.5	50
2		9.7 \pm 0.3	18.5 \pm 1.0	< 10
3		11.0 \pm 0.7	6.0 \pm 1.3	< 5
4		6.4 \pm 0.2	10.6 \pm 0.5	< 10

Note: NAT inhibitors were identified through a high-throughput screen of a 5000-strong library of drug-like small molecules (Russell et al., 2009) with a panel of three pure recombinant prokaryotic NAT enzymes (NATs from *Mycobacterium smegmatis*, *Salmonella typhimurium* and *Pseudomonas aeruginosa*) and two eukaryotic NAT enzymes (human NAT1 and hamster NAT2). The minimum inhibitory concentration (MIC) values against *Mycobacterium tuberculosis* H₃₇Rv of NAT inhibitors identified from the high-throughput screen were determined as described (Anderton et al., 2006). Determinations of IC₅₀ values with pure recombinant PANAT and MMNAT were determined for compounds **1–3** with 5-aminosalicylate as substrate and compound **4** with anisidine.

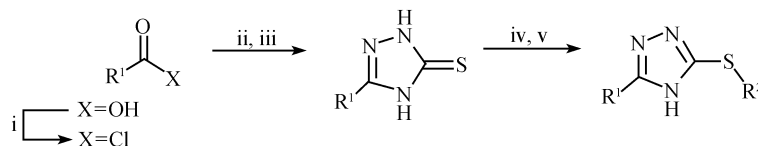


Scheme 1. Reagents and conditions for production of 4. i, pyridine, RT, 4 h; ii, NaHCO₃ (1 M, aq.), 100°C, 16 h; iii, BrCH₂CH₂COOMe (1.2 eq.), polymer-supported methylmorpholine (1.2 eq.), DMF, RT, 72 h. ^a purity was determined by RP-HPLC.

methylthiourea (for activated electrophiles) or polymer-supported thiophenolate (for non-activated electrophiles) furnished the S-substituted 1,2,4-triazoles **13–18** in 18%–45% isolated yield and >95% purity (Table 2).

Compound **4** exhibited competitive inhibition of NAT with respect to the substrate *p*-anisidine (ANS) at inhibitor

concentrations of up to 10 μ M (Fig. 3A) and the inhibition constant, K_{ic} , was found to be 6.0 \pm 0.3 μ M (Fig. 3B). The synthetic precursor to compound **4**, 1,2,4-triazole-3-thione, **5**, showed very similar inhibitory properties (Table 2) with competitive inhibition at concentrations up to 10 μ M, with a K_{ic} value of 8.6 \pm 0.5 μ M.



Scheme 2. Synthesis of 3,5-disubstituted 1,2,4-triazoles. Reagents and conditions: i, SOCl_2 , 70°C , 1 h; ii, $\text{H}_2\text{NNHCSNH}_2$, pyridine, RT, 4 h; iii, NaHCO_3 (1 M, aq.), 100°C , 16 h; iv, R^2X (1.2 eq.), PS-methylmorpholine, DMF, RT, 72 h; v, PS-thiophenol, 50°C , 16 h, or PS-methylthiourea, 60°C , 4 h.

Table 2 Biological activity of 3,5-disubstituted 1,2,4-triazoles

product	R^1	R^2	yield (%) ^a	purity ^b	IC_{50} against NAT (μM)
4	4-MeC ₆ H ₄	(CH ₂) ₂ CO ₂ Me	32	> 95	6.4 ± 0.2
5	4-MeC ₆ H ₄	H	62	> 95	1.40 ± 0.54
6	4-MeC ₆ H ₄	(CH ₂) ₂ CO ₂ H	77	> 95	20.1 ± 0.9
7	C(CH ₃) ₃	H	8	> 95	> 50
8	4-MeOC ₆ H ₄	H	98	> 95	9.0 ± 1.0
9	4-ClC ₆ H ₄	H	96	> 95	14.0 ± 0.5
10	3-ClC ₆ H ₄	H	44	> 95	0.244 ± 0.030
11	3,4-Cl ₂ C ₆ H ₃	H	92	> 95	2.66 ± 0.11
12	3-Cl-4-MeOC ₆ H ₃	H	29	> 95	1.9 ± 0.2
13	4-MeC ₆ H ₄	Me	67	> 95	> 50
14	4-MeC ₆ H ₄	(CH ₂) ₂ Me	67	> 95	> 50
15	4-MeC ₆ H ₄	CH ₂ C ₆ H ₅	97	> 95	29.9 ± 2.7
16	4-MeC ₆ H ₄	CH ₂ (4-C ₆ H ₄ Ph)	7	> 95	5.18 ± 0.7
17	4-MeC ₆ H ₄	(CH ₂) ₇ Me	23	> 95	3.82 ± 0.37
18	4-MeC ₆ H ₄	(CH ₂) ₉ Me	32	> 95	13.1 ± 1.1

^a Overall yield from starting carboxylic acid or acid chloride.

^b Purity determined by RP-HPLC. NAT assays with the pure recombinant NAT from *P. aeruginosa* were performed with anisidine as substrate as described in the Materials and Methods.

An aryl substituent at the C5 position on the 1,2,4-triazole ring was found to be essential for inhibition of NAT. For example, 5-*tert*-butyl-1,2,4-triazole-3-thione (**7**) showed no inhibition of NAT activity at any concentration tested (up to $50 \mu\text{M}$, Table 2). Of the 5-aryl-1,2,4-triazoles synthesised, the 4'-methoxyphenyl (**8**) and 4'-chlorophenyl (**9**) derivatives were considerably less active as NAT inhibitors than the parent and precursor 4'-methylphenyl compounds, **4** and **5** (Table 2). However, the 3'-chlorophenyl-1,2,4-triazole-3-thione (**10**) showed an increase in activity as a NAT inhibitor relative to the 4'-methylphenyl triazole, with an IC_{50} value of $244 \pm 30 \text{ nM}$, a 60-fold increase in potency. However, the compounds that possessed a nucleophilic sulfur (where substituent R^2 is H, **5**, **7–12**, Table 2) while not observed to react with DTNB or Coenzyme A, were not pursued further due to their potential non-selective reactivity with intracellular electrophiles.

In exploring the preliminary structure-activity relationships for NAT ligands (Brooke et al., 2003a, b), we observed that the incorporation of a large hydrophobic substituent markedly

improved the ligand potency. To probe this effect further, a series of 1,2,4-triazoles with long chain aliphatic or planar aromatic substituents on sulfur were evaluated. Clear structure-activity relationships could be ascertained among these compounds. The length of the chain of the S-substituent was estimated following energy minimization with Chem3D Pro (Cambridgesoft). The assumption was made that the carbon chain exists in an extended conformation where multiple conformations are accessible. The NAT inhibition potency increased with extended chain length up to approximately 10 \AA , with the S-4-phenylbenzyl (**16**) and S-octyl (**17**) derivatives being the most potent in the series (Fig. 4A). The S-decyl derivative **18** has an approximate chain length of 13 \AA and was a less potent inhibitor of NAT than the shorter-chain S-alkyl derivatives. The IC_{50} against NAT of the S-decyl derivative (**18**) was $13.1 \pm 1.1 \mu\text{M}$, compared with an IC_{50} of $3.8 \pm 0.4 \mu\text{M}$ for the S-octyl-1,2,4-triazole (**17**).

The simulated annealing of compound **4** and its structural analogs to NAT from *M. tuberculosis* was then evaluated by docking with the program GOLD (Verdonk et al., 2003). The

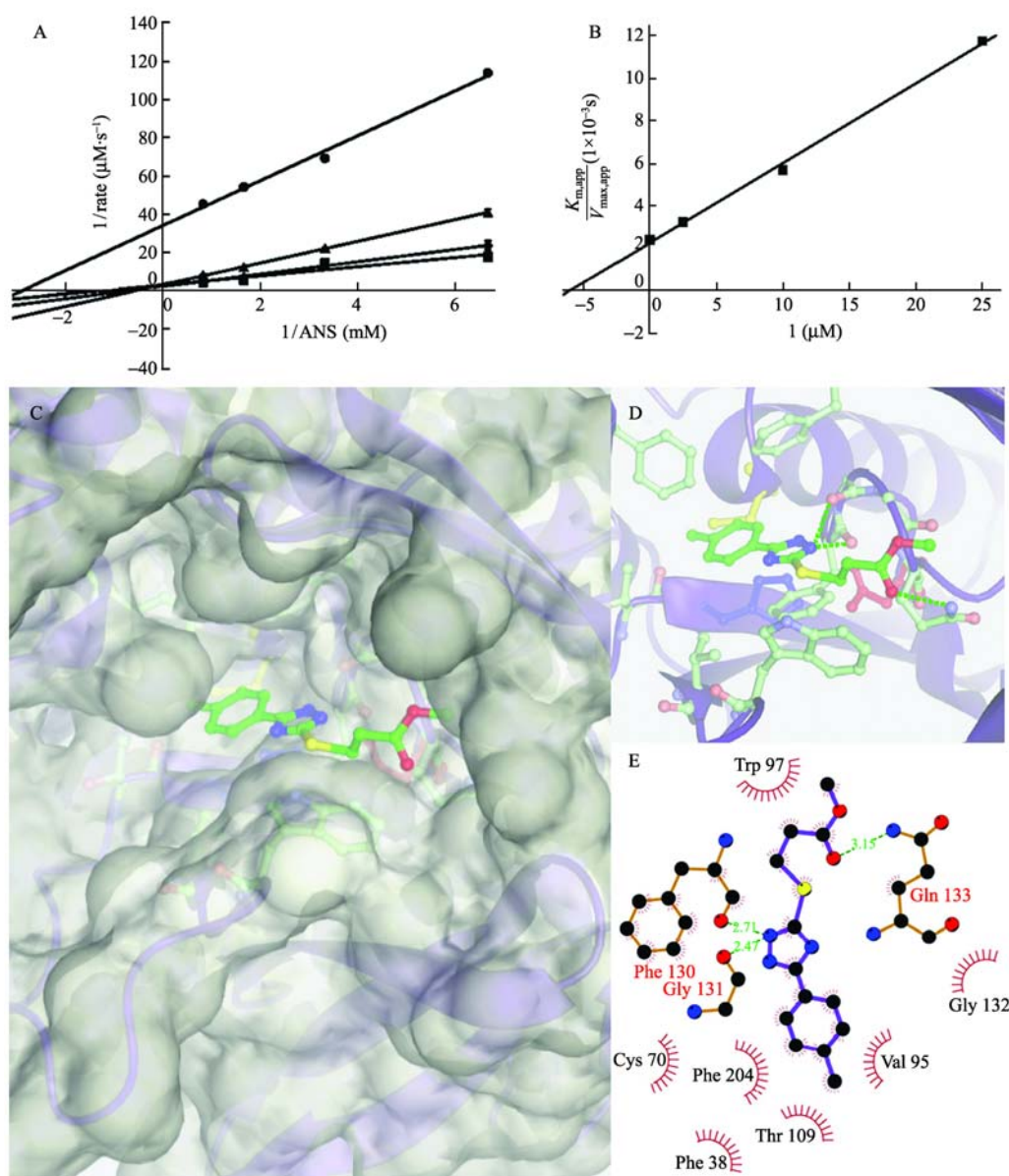


Figure 3. The inhibition with substrate 4-anisidine (ANS) and the molecular docking of compound 4. (A) Lineweaver-Burk plot showing inhibition of PANAT by compound 4 with the substrate 4-anisidine (ANS). The y-coordinate shows the reciprocal rate of reaction, measured by determining the rate of production of CoA as described previously (Brooke et al., 2003a). The x-coordinate shows the reciprocal of the substrate concentration. The concentration of inhibitor was varied: 0 (squares), 2.5 μM (diamonds), 10 μM (triangles), or 25 μM (circles). Each point represents the mean \pm S.D. from triplicate determinations. The y-intercept gives $1/V_{\text{max},\text{app}}$, the slope of each line gives $K_{m,\text{app}}/V_{\text{max},\text{app}}$ and the x-intercept gives $-1/K_{m,\text{app}}$. (B) Secondary plot of $K_{m,\text{app}}/V_{\text{max},\text{app}}$ on the y-coordinate against inhibitor concentration on the x-coordinate. For competitive and mixed types of inhibition, the slope of the line gives K_{m}/V_{max} and the y-intercept gives $K_{m}/(V_{\text{max}} \times K_{ic})$ (Cornish-Bowden, 1995), from which the pure competitive inhibition constant, K_{ic} , was found to be $6.0 \pm 0.3 \mu\text{M}$. (C) and (D) The lowest-energy docking solution for compound 4 with the TBNAT model, as described in Materials and Methods. The protein secondary structure is represented beneath the surface and compound 4 is shown in ball and stick representation. Predicted hydrogen bonds are shown in green. (E) A two-dimensional representation of the binding of 4 to TBNAT. The figure was prepared with LigPlot (Wallace, 1995). Hydrogen bonds are shown in green with calculated distances expressed in Å. Red dashes indicate hydrophobic interactions between protein residues and the ligand. All of the contact residues identified between compound 4 and the *M. tuberculosis* NAT protein are conserved between *M. marinum* NAT and *M. tuberculosis* NAT, except for Gln¹³³ (in *M. tuberculosis* NAT), which is a Met residue in *M. marinum* NAT. All of the side-chains are in essentially identical orientations between the two protein structures.

NATs from *M. marinum* and *M. tuberculosis* share 74% identity and 83% similarity at the amino acid level (Fullam et al., 2007), and the root mean square deviation between the 1080 backbone peptide atoms of the crystal structure of *M. marinum* NAT and the equivalent atoms in the model of *M. tuberculosis* NAT is 0.48 Å. The predicted binding orientation of **4** into the NAT from *M. tuberculosis* is shown in Fig. 3. The triazole ring was predicted to form π -stacking interactions with Phe¹³⁰, and to form H-bonds with the backbone carbonyls of Phe¹³⁰ and Gly¹³¹, residues in the proposed 'P-loop' (Sinclair et al., 2000). The carbonyl of the ester moiety of **4** is in position to H-bond with Gln¹³³. These anchor points result in the orientation of the 4'-methylphenyl moiety towards the active site Cys⁷⁰ residue, in a hydrophobic pocket bounded by Phe³⁸, Phe²⁰⁴, Val⁹⁵ and Thr¹⁰⁹. The correlation observed between chain length and NAT inhibitory potency (Fig. 4) was

closely matched by the docking scores for the same series of compounds (Fig. 5). An increase in the calculated binding affinity was observed in the series: S-methyl (**13**), S-propyl (**14**), S-benzyl (**15**), S-4-phenylbenzyl (**16**) and S-octyl (**17**) 1,2,4-triazoles. When the S-substituent was a decyl chain (**18**), the docking score was lower than for the S-octyl derivative. Fig. 5 shows the relative binding orientations of this series of 1,2,4-triazoles, with compound **4** included for comparison. All except compound **18** were predicted to bind in essentially identical orientations. The major predicted binding interactions between these compounds and the *M. tuberculosis* NAT protein were very similar to those described above for compound **4**: π -stacking of the 1,2,4-triazole ring with Phe¹³⁰ and H-bonding of one nitrogen of the 1,2,4-triazole ring with the carbonyl oxygens of the 'P-loop' residues, Phe¹³⁰ and Gly¹³¹ (Sinclair et al., 2000). The 4'-

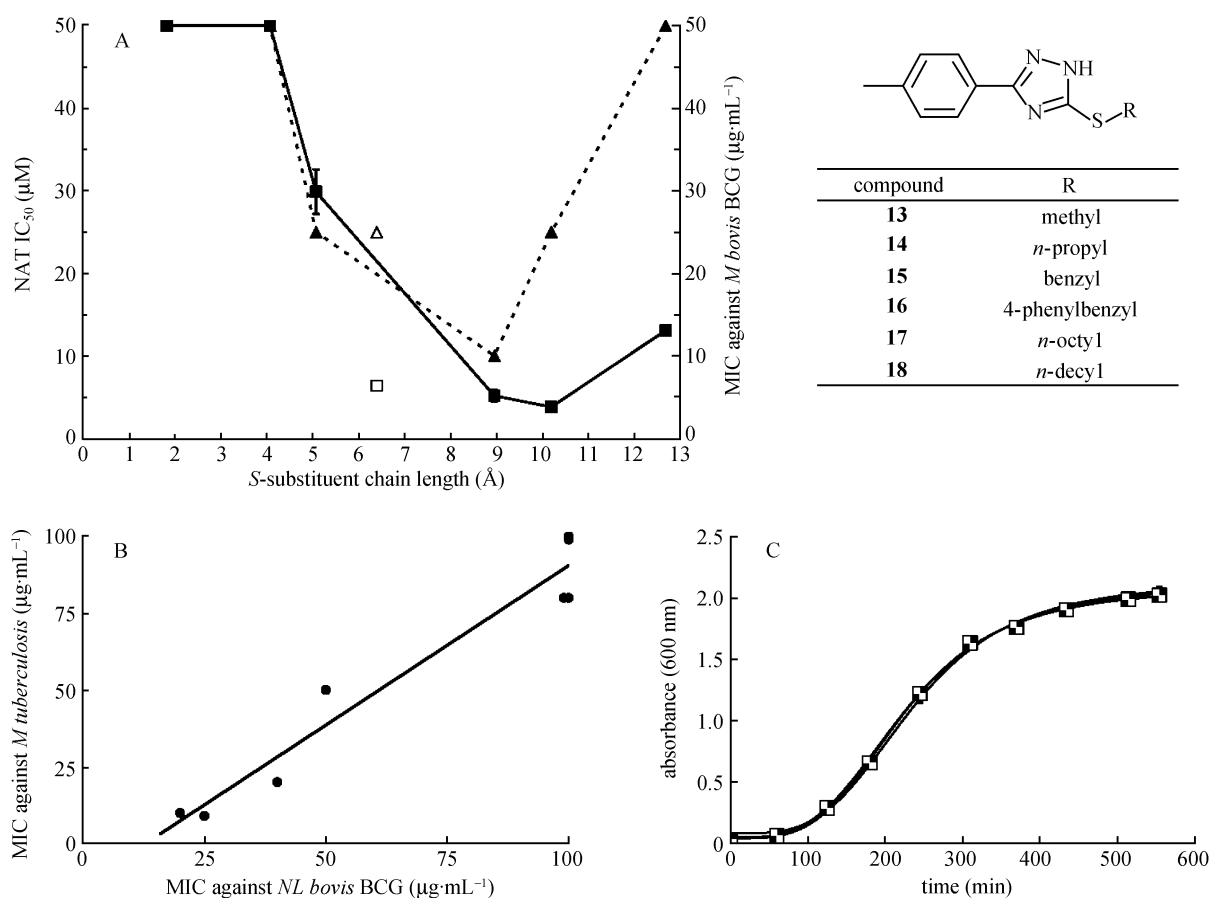


Figure 4. The inhibitory effects of 1,2,4-triazole series. (A) Correlation of the growth inhibition of *M. bovis* BCG and the inhibition of NAT activity with the S-substituent chain length of a series of S-alkyl 1,2,4-triazoles. For each compound in the series, the IC₅₀ (■) of the compound with NAT from *P. aeruginosa* was determined as previously described (Brooke et al., 2003a). The minimum inhibitory concentration (MIC), determined as previously described with *M. bovis* BCG (Anderton et al., 2006) is also shown (▲). Compound **4** is included for comparison (open symbols). Approximate chain lengths of alkyl and aryl S-substituents were calculated with Chem3D (Cambridgesoft) after energy-minimization with the MM2 force field. (B) Correlation between the growth inhibition of *M. bovis* BCG and *M. tuberculosis* H37Rv. Each data point represents one compound from the 1,2,4-triazole series. (C) Growth of *E. coli* in the presence of 1,2,4-triazole inhibitors (at 100 $\mu\text{g mL}^{-1}$): compound **4** or a DMSO-only control. The best-fit lines for all growth curves are shown and overlapping data points are marked as chequered squares.

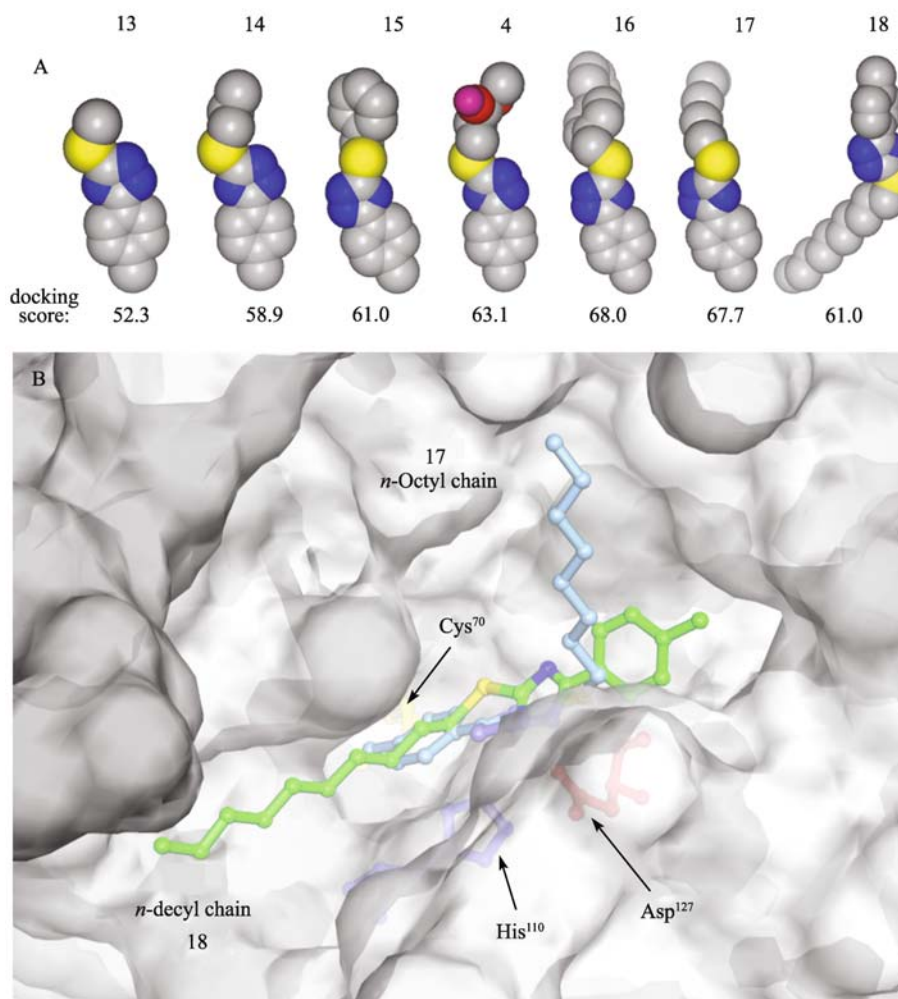


Figure 5. Molecular docking of S-substituted 1,2,4-triazoles with NAT from *M. tuberculosis*. (A) The space-filling representations of the lowest-energy docking solutions of the S-hydrocarbon substituted 1,2,4-triazoles in identical relative orientations, after docking into *M. tuberculosis* NAT. Compound **4** is included for comparison. Docking was performed as described in Materials and Methods, and the GoldScore fitness (docking score) is shown for each compound. The figure was prepared with MarvinSpace, version 1.2 (ChemAxon, Budapest, Hungary. www.chemaxon.com). (B) An overlay of the docking solutions for compounds **17** (blue) and **18** (green) relative to the active site of the *M. tuberculosis* NAT protein. The active-site catalytic-triad residues—Cys⁷⁰ (yellow), His¹¹⁰ (blue) and Asp¹²⁷ (red)—are shown underneath the calculated molecular surface of the *M. tuberculosis* NAT protein structure. The docking results predict that the S-decyl derivative (**18**) cannot occupy the same relative orientation as the smaller S-substituted compounds, such as the S-octyl 1,2,4-triazole, **17** (B), due to the size of the active site. With the exception of compound **18**, the 4-methylphenyl group common to this series is positioned close to the active site Cys⁷⁰ residue, deep in the active site pocket. A comparison of the predicted contact residues in *M. marinum* NAT with the equivalent residues of *M. tuberculosis* NAT is shown in Supplementary Figure. Two of the seventeen contact residues are not identical between the proteins: Gln¹³³ and Ala¹⁹⁶ in *M. tuberculosis* NAT are Met¹³³ and Val¹⁹⁶ respectively in *M. marinum* NAT.

methylphenyl group in all molecules (except the S-decyl derivative **18**) was predicted to point towards the active site cysteine residue, as described for **4**, above.

Inhibition of growth of *M. bovis* BCG and *M. tuberculosis*

The series of 1,2,4-triazole-3-thiones was tested for inhibitory effects on the growth of *M. bovis* BCG and *M. tuberculosis*

H37Rv. There was excellent correlation between the inhibitory effects on the growth of both organisms (Fig. 4B), and for all compounds there appeared to be greater potency in inhibition of *M. tuberculosis* growth. The growth inhibitory effects were specific, since there was no inhibition of growth of *E. coli* cultures at up to 100 µg/mL (Fig. 4C). Compound **4** was a modestly potent inhibitor of both NAT activity and the growth of mycobacteria. The relationship between inhibition

of NAT activity and inhibition of growth of *M. bovis* BCG by compound **4** and its structural analogs was investigated. Carboxylic acid **6** was an inhibitor of the NAT enzyme *in vitro*. However, **6** was found not to be an inhibitor of mycobacterial growth. This may be due to poor cell wall permeability of the carboxylate salt of **6**, which is expected to be the predominant form of **6** under the assay conditions. In contrast, there was good correlation between inhibitory potency against NAT and mycobacterial growth inhibition for the remaining S-substituted analogues of compound **4** (Fig. 4). Inhibitory activities on both the NAT enzyme and on growth of *M. bovis* BCG were affected similarly by the length of the S-substituent, with maximum inhibition corresponding to an extended chain length of around 9 to 10 Å.

NAT inhibitors mimic the effects of Δnat strain

Compound **4**, which is a competitive inhibitor of NAT at less than 10 μ M, was a good inhibitor of the growth of *M. bovis* BCG on agar. Treatment of *M. bovis* BCG with compound **4** resulted in a major effect on the lipid composition (Fig. 6C–E). The effect was very similar to that observed when the *nat* gene was deleted (Bhakta et al., 2004): there was a diminution in the amount of the mycolic acids and complex lipids, although the phospholipid composition appeared to be relatively unchanged (Fig. 6). In addition, it was observed that compound **4** acted synergistically with gentamycin, mimicking the effect of the genetic deletion of *nat* in *M. bovis* BCG. Gentamycin alone is not inhibitory against the growth of wild-type *M. bovis* BCG at 10 μ g/mL (Fig. 6B), but does affect the growth of the Δnat strain of *M. bovis* BCG at 10 μ g/mL (Bhakta et al., 2004).

In order to determine whether NAT inhibitors would also be active on the intracellular growth of *M. bovis* BCG, the effects were tested initially on macrophages alone. Compound **4** was not toxic to macrophages (Fig. 6F). However, when macrophage were infected with *M. bovis* BCG that had been exposed to compound **4**, the bacilli were killed within the macrophage, as has been demonstrated with the Δnat strain (Fig. 6G) (Bhakta et al., 2004). The same effects were observed at the highest concentration when compound **4** was added after the macrophages had been infected (data not shown).

DISCUSSION

There is an urgent need for novel therapies for tuberculosis, and here we report a new potential drug target in *M. tuberculosis*: the arylamine *N*-acetyltransferase enzyme. Following from previous work on genetic deletion of the *nat* gene in *M. bovis* BCG (Bhakta et al., 2004), we now report on the identification and anti-mycobacterial activity of novel small-molecule inhibitors of NATs. From high-throughput screening, we have identified four compounds from

chemically distinct structural classes that are active both as inhibitors of purified prokaryotic NAT enzymes and as inhibitors of the growth of *M. tuberculosis*.

We have synthesised an array of analogs of one of these high-throughput screening hits, the 1,2,4-triazole **4**. Structure-activity relationships were identified for a series of S-substituted 1,2,4-triazole-3-thiones where the S-substituent was an aliphatic or planar aromatic group. These structure-activity relationships show that the maximal NAT inhibitory activity occurs when the S-substituent extended chain length is around 9–10 Å (Fig. 4). A similar pattern of interaction between a series of substrates (4-alkoxyanilines) and NAT from *M. smegmatis* has also been observed (Brooke et al., 2003b). These NAT substrates/ligands were shown to have anti-tubercular activity although by an unexplained mechanism (Nodzu et al., 1954). For the 1,2,4-triazole series described (Table 2, Fig. 4), the increase in alkyl chain length allows for more enthalpically favorable hydrophobic contacts within the active site, at the expense of an increasing entropic penalty for binding to the protein. The *in silico* docking experiments successfully predict the observed structure-activity relationships for the 1,2,4-triazole series (Fig. 5), and provide a rationale for the observed trends in decreased NAT inhibitory potency when the alkyl chain length is ten carbon units. Binding energy is most favorable and NAT inhibitory potency is maximal when the chain length is equivalent to eight carbons. Furthermore, the structure-activity relationships observed for inhibition of mycobacterial growth mirrored those for NAT inhibition. The availability of NAT inhibitors also allows for studies to investigate the role of NAT in mycobacterial cell wall synthesis and we are pursuing both the class that we describe here and the other classes of inhibitor that we have identified.

Recently, efficient methods for generating sufficient amounts of the NAT enzyme from *M. tuberculosis* have been identified (Sikora and Blanchard, 2008; Fullam et al., 2009) and the enzyme shows a very similar substrate specificity profile to the NAT enzyme from *M. marinum* (Fullam et al., 2009). The studies presented here where NAT has been used in a high-throughput screen have identified compounds that have anti-tubercular activity and the triazoles affect mycobacteria within macrophage. These studies also demonstrate an inhibitory effect on growth on agar, whilst the *nat* deleted mutant strain of *M. bovis* BCG does show slower growth. Although the *nat* gene does not appear to be essential for growth on agar, it does appear to be essential for survival of *M. bovis* BCG inside macrophage. Whilst these studies do not eliminate the possibility that the inhibitors may also act against an additional target in mycobacteria, they suggest that this approach has identified a novel series of compounds to pursue as anti-tubercular agents. The recent finding that the other genes of the operon in which NAT is encoded are essential for survival *in vivo* (Yam et al., 2009) and the observation of the role of the gene

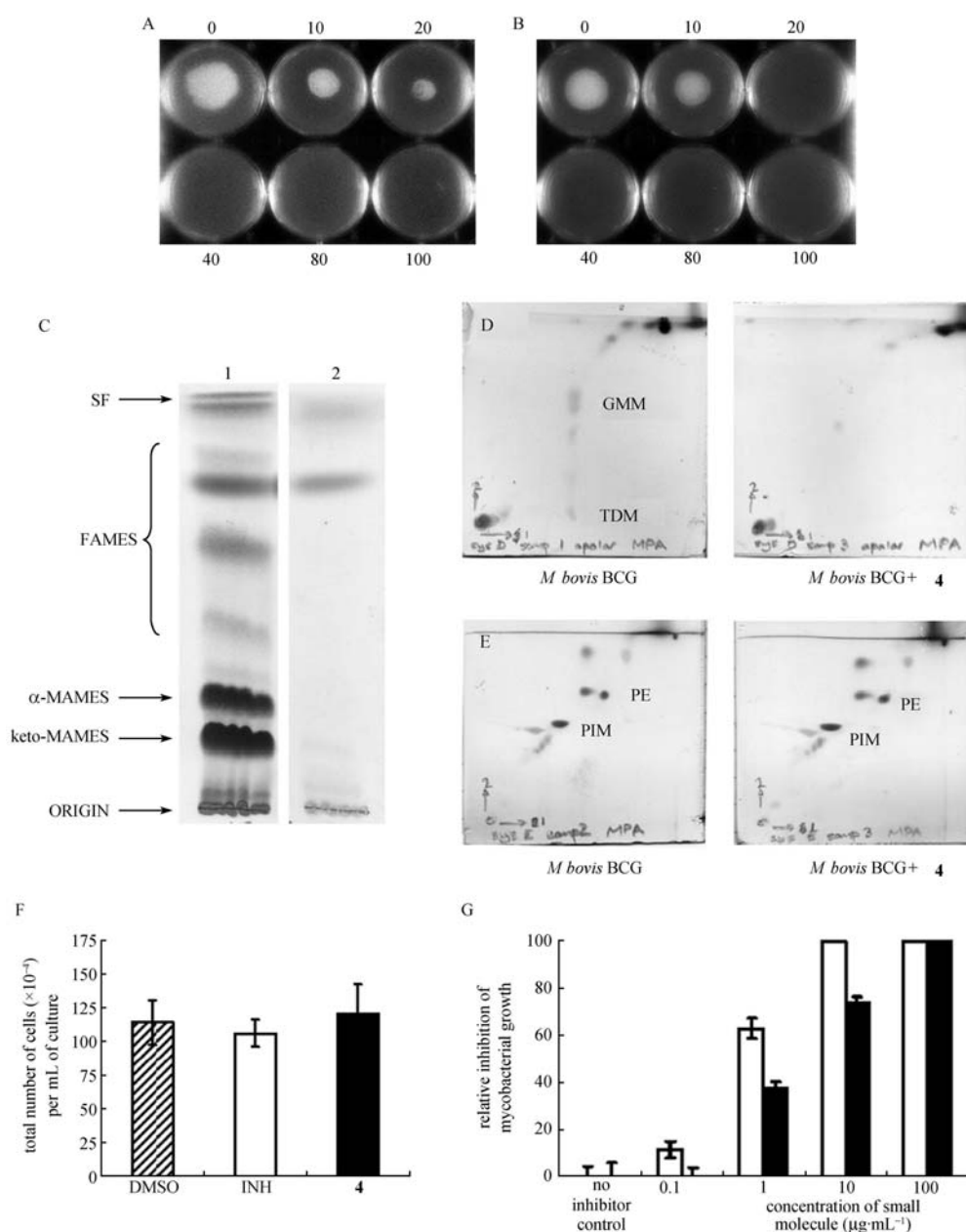


Figure 6. Effect of NAT inhibitors on the growth of mycobacteria. (A) *M. bovis* BCG cultures grown in the presence of compound 4 at the concentrations indicated (from 0 to 100 µg/mL in each well). The experimental procedure is described in Materials and Methods. (B) *M. bovis* BCG with 4 as in (A) but also with gentamycin in each well at a concentration of 10 µg/mL, including the well (0) with DMSO and no compound 4. (C–E) The mycolate profile of *M. bovis* BCG is altered when grown in liquid culture in the presence of 4 at a concentration of 20 µg/mL. Cells were harvested at mid-exponential phase of growth (optical density at 600 nm = 1.0). Lipid extractions and analyses were carried out with an equivalent biomass of each sample as previously described (Besra, 1998). The alpha- and keto-mycolic acid methyl esters (MAMES) of *M. bovis* BCG (C, lane 1) or *M. bovis* BCG grown in the presence of 4 (C, lane 2) were analyzed by thin layer chromatography (TLC). Fatty acid methyl esters (FAMES), solvent front (SF) and the origin are indicated. The extracted lipids were also analyzed by two-dimensional TLC with different solvent systems ('D1' and 'E'), as previously described (Besra, 1998). (D) 2D-TLC plates showing the apolar lipid components run in solvent system 'D1' (Besra, 1998). Spots corresponding to trehalose dimycolate (Cord Factor, TDM) and glucose monomycolate (GMM) were not present in the lipid extract from *M. bovis* BCG cells grown in the presence of compound 4. (E) 2D-TLC plates showing the polar lipids run in solvent system 'E' (Besra, 1998). No effect of compound 4 was observed on the levels of phospholipids (PE, phosphatidylethanolamine; PIM, phosphatidylinositolmannosides). (F) and (G) Compound 4 is not toxic to macrophage RAW 264.7 cells but enhances the killing of *M. bovis* BCG inside mouse macrophages (RAW 264.7). (F) RAW 264.7 cells were grown in RPMI in the presence of compound 4 (black bars) at 50 µg/mL in DMSO for 72 h at 37°C in a 5% CO₂ incubator. The anti-tubercular drug INH (white bars) was included as a control at a concentration of 50 µg/mL, and a control was included with DMSO alone (hatched bars). In all samples, the final concentration of DMSO was 0.1%. (G) The concentration-dependent effect of compound 4 and INH on the intracellular survival of *M. bovis* BCG in macrophage cells. The experiment was conducted as described in Materials and Methods. The relative inhibition of growth by 4 and INH was determined by CFU counting and was compared to controls in which DMSO only was added. The final concentration of DMSO in all experiments was 0.1% (v/v). An inhibition of 100% represents no CFUs after incubation of the lysed RAW 264.7 cell contents at 37°C for 21 days.

cluster in cholesterol metabolism (van der Giese et al., 2007; Lack et al., 2009) controlled by the KstR regulon (Kendall and Stoker, 2007) further underline the importance of this group of genes as targets for exploring anti-tubercular agents.

There is a move to identify compounds that affect more than one target and, in the fight against TB, potentially useful targets should not be ignored, especially when the target is important for intracellular survival of mycobacteria within macrophage.

MATERIALS AND METHODS

Protein production and enzymic assays

The NAT enzymes from *M. smegmatis* (Payton et al., 1999), *S. typhimurium* (Sinclair et al., 2000), *P. aeruginosa* (Westwood et al., 2005), *M. marinum* (Fullam et al., 2007), hamster NAT2 (Kawamura, 2005) and human NAT1 (Wang, 2005) were produced as recombinant proteins and purified as previously described. Activity assays were performed as previously described (Kawamura, 2005; Brooke, 2003a, b).

Computational docking of inhibitors with NAT

The program Modeller 8v2 (Sali and Blundell, 1993) was used to construct a model of the TBNAT protein from the known crystal structures of NATs from *M. smegmatis* (PDB code 1GX3) (Sandy et al., 2002), *S. typhimurium* (PDB code 1E2T) (Sinclair et al., 2000), *M. marinum* (PDB code 2VFB), *P. aeruginosa* (PDB code 1W4T) (Westwood et al., 2005) and *Mesorhizobium loti* NAT1 (PDB code 2BSZ) (Holton et al., 2005). A comparison of the model with *M. marinum* NAT (PDB code 2VFB) is shown in Supplementary Fig. 1. The protein file was prepared in pdb format by using the AddH tool within the Chimera molecular modeling package (Pettersen et al., 2004), and docking was performed with GOLD v3.0.1 (Verdonk et al., 2003). Ligand structures were drawn in ChemDraw (Cambridgesoft) and then converted to 3-dimensional structures in Chem3D. The molecules were energy-minimized with the MM2 force field and saved in sdf format for docking. The active site of the protein was defined by the Sy atom of Cys⁷⁰ with an automatic cavity-detection radius of 20 Å. The docking solutions were ranked with the GoldScore algorithm. Lowest-energy docking solutions were merged with the protein structure and saved in the pdb format, prior to visualization with Aesop as previously described (Sinclair et al., 2000).

Mycobacterial growth inhibition *in vitro*

Mycobacteria (*M. bovis* BCG and *M. tuberculosis* H37Rv) were grown as spot cultures in 6-well plates on solid medium (Middlebrook 7H10 medium supplemented with 10% (v/v) oleic acid-albumin-dextrose-catalase (OADC)) as previously described (Anderton et al., 2006), with test compounds at the concentrations indicated in the text. Test compounds were added to the melted, partially cooled 7H10-OADC agar medium as solutions in DMSO, and the final concentration of DMSO in each well was 0.1% (v/v). The minimum inhibitory concentration (MIC) is defined as the concentration of inhibitor at which no growth of mycobacteria was detected after a period of 2–3 weeks.

Effect of NAT inhibitors on the infection of macrophages by *M. bovis* BCG

M. bovis BCG was grown for approximately 4 days in 7H9 medium (containing 10% (v/v) albumin-dextrose-catalase (ADC), 0.2% (v/v) glycerol and 0.05% (v/v) Tween-80) until the optical density at 600 nm was 1.0. The mycobacterial cells were washed and resuspended in 7H9-ADC medium (as above) supplemented with compound **4** (at 20 µg/mL) or isoniazid (INH) (0.01 µg/mL) in DMSO at a final concentration of 0.1% (v/v). A control was included where DMSO alone was used. After incubation with the test compound for 2 h, the mycobacterial cells were washed and resuspended in RPMI (containing 0.05% Tween-80) for infection of RAW 264.7 mouse macrophages. The RAW 264.7 cells were grown routinely in RPMI medium (supplemented with 10% (v/v) fetal bovine serum (FBS)) without antibiotics for 48 h at 37°C in a humidified, 5% CO₂ atmosphere prior to the infection. RAW 264.7 cells (5 × 10⁴ per well) were seeded onto 24-well tissue-culture plates and incubated (at least 30 minutes) with the test compound (at the concentrations shown in Fig. 5G) or DMSO alone, prior to infection with *M. bovis* BCG (5 × 10⁵ mycobacterial cells per well, prepared as described above). After 2 h, the adherent RAW 264.7 cells were washed twice with RPMI, and then resuspended in RPMI containing test compound or DMSO alone (at the concentrations shown in Fig. 5G). The infected RAW 264.7 cells were cultured for 72 h in RPMI-FBS medium containing either the test compounds or vehicle alone and then washed twice with RPMI alone and lysed by the addition of sterile water. The surviving *M. bovis* BCG cells in the lysed RAW 264.7 cell suspension were cultured on 7H10-OADC agar medium for 3 weeks at 37°C. The number of colony forming units (CFUs) in each case was determined and used for comparison between tests and controls.

Chemical methods: synthesis and characterization data

See supplementary information.

ACKNOWLEDGEMENTS

The authors thank Hilary Long for excellent technical assistance, Dr Kerry Millington for helpful discussions and Ornella Sciuto for help in preparing the manuscript. We thank the Wellcome Trust and the Medical Research Council for financial support.

ABBREVIATIONS

acetylCoA, acetyl Coenzyme A; ANS, anisidine; DMSO, dimethylsulfoxide, DTNB, 5,5'-dithio-bis(2-nitrobenzoic acid); MIC, minimum inhibitory concentration; IC₅₀, concentration of inhibitor showing 50% inhibition compared with solvent only as 100% activity; INH, isoniazid; PANAT, pure recombinant NAT enzyme from *Pseudomonas aeruginosa*; MSNAT, pure recombinant NAT enzyme from *Mycobacterium smegmatis*; NAT, arylamine N-acetyltransferase; STNAT, pure recombinant NAT enzyme from *Salmonella typhimurium*; MMNAT, pure recombinant NAT enzyme from *Mycobacterium marinum*; HNAT1, pure recombinant human NAT1 enzyme; shNAT2, pure recombinant hamster NAT2 enzyme; TB, tuberculosis

REFERENCES

- Al-Balas, Q., Anthony, N.G., Al-Jaidi, B., Alnimr, A., Abbott, G., Brown, A.K., Taylor, R.C., Besra, G.S., McHugh, T.D., Gillespie, S.H., *et al.* (2009). Identification of 2-aminothiazole-4-carboxylate derivatives active against *Mycobacterium tuberculosis* H37Rv and the beta-ketoacyl-ACP synthase mtFabH. *PLoS ONE* 4, e5617.
- Anderton, M.C., Bhakta, S., Besra, G.S., Jeavons, P., Eltis, L.D., and Sim, E. (2006). Characterization of the putative operon containing arylamine N-acetyltransferase (nat) in *Mycobacterium bovis* BCG. *Mol Microbiol* 59, 181–192.
- Besra, G.S. (1998). Preparation of cell-wall fractions from mycobacteria. *Methods Mol Biol* 101, 91–107.
- Bhakta, S., Besra, G.S., Upton, A.M., Parish, T., Sholto-Douglas-Vernon, C., Gibson, K.J., Knutton, S., Gordon, S., DaSilva, R.P., Anderton, M.C., *et al.* (2004). Arylamine N-Acetyltransferase Is Required for Synthesis of Mycolic Acids and Complex Lipids in *Mycobacterium bovis* BCG and Represents a Novel Drug Target. *J Exp Med* 199, 1191–1199.
- Brooke, E.W., Davies, S.G., Mulvaney, A.W., Pompeo, F., Sim, E., and Vickers, R.J. (2003a). An approach to identifying novel substrates of bacterial arylamine N-acetyltransferases. *Bioorg Med Chem* 11, 1227–1234.
- Brooke, E.W., Davies, S.G., Mulvaney, A.W., Okada, M., Pompeo, F., Sim, E., Vickers, R.J., and Westwood, I.M. (2003b). Synthesis and in vitro evaluation of novel small molecule inhibitors of bacterial arylamine N-acetyltransferases (NATs). *Bioorg Med Chem Lett* 13, 2527–2530.
- Cole, S.T., Brosch, R., Parkhill, J., Garnier, T., Churcher, C., Harris, D., Gordon, S.V., Eiglmeier, K., Gas, S., Barry, C.E., 3rd, *et al.* (1998). Deciphering the biology of *Mycobacterium tuberculosis* from the complete genome sequence. *Nature* 393, 537–544.
- Cole, S.T., and Alzari, P.M. (2005). Microbiology. TB—a new target, a new drug. *Science* 307, 214–215.
- Dhiman, R.K., Mahapatra, S., Slayden, R.A., Boyne, M.E., Lenaerts, A., Hinshaw, J.C., Angala, S.K., Chatterjee, D., Biswas, K., Narayanasamy, P., *et al.* (2009). Menaquinone synthesis is critical for maintaining mycobacterial viability during exponential growth and recovery from non-replicating persistence. *Mol Microbiol* 72, 85–97.
- Diacon, A.H., Pym, A., Grobusch, M., Patientia, R., Rustonjee, R., Page-Shipp, L., Pistorius, C., Krause, R., Bogoshi, M., Churchyard, G., *et al.* (2009). The diarylquinoline TMC207 for multidrug-resistant tuberculosis. *N Engl J Med* 360, 2397–2405.
- Dye, C. (2006). Global epidemiology of tuberculosis. *Lancet* 367, 938–940.
- Evans, D.A., Manley, K.A., and McKusick, V.A. (1960). Genetic control of isoniazid metabolism in man. *Br Med J* 5197, 485–491.
- Foroumadi, A., Kargar, Z., Sakhteman, A., Sharifzadeh, Z., Feyzmohammadi, R., Kazemi, M., and Shafiee, A. (2006). Synthesis and antimycobacterial activity of some alkyl [5-(nitroaryl)-1,3,4-thiadiazol-2-ylthio]propionates. *Bioorg Med Chem Lett* 16, 1164–1167.
- Fullam, E., Westwood, I.M., Anderton, M.C., Lowe, E.D., Sim, E., and Noble, M.E.M. (2007). Divergence of cofactor recognition across evolution: Coenzyme A binding in a prokaryotic arylamine N-acetyltransferase. *J Mol Biol* 375, 178–191.
- Fullam, E., Kawamura, A., Wilkinson, H., Abuhammad, A., Westwood, I., and Sim, E. (2009). Comparison of the Arylamine N-acetyltransferase from *Mycobacterium marinum* and *Mycobacterium tuberculosis*. *Protein J* 28, 281–293.
- Holton, S.J., Dairou, J., Sandy, J., Rodrigues-Lima, F., Dupret, J.M., Noble, M.E., and Sim, E. (2005). Structure of *Mesorhizobium loti* arylamine N-acetyltransferase 1. *Acta Crystallogr C* 61, 14–16.
- Jacobson, R., Ramsay, J., Aller, H. and Thirugnanam, M. (1987). 1-Dimethylcarbamoyl-3-substituted-5-substituted-1H-1,2,4-triazoles. European Patent Office, EP0213718.
- Jeney, E., and Zsolnai, T. (1956). Studies in search of new tuberculostatic drugs. I. Hydrazine derivatives, carbolic acid, phenols, quaternary ammonium compounds and their intermediaries. *Zentralblatt für Bakteriologie, Parasitenkunde, Infektionskrankheiten und Hygiene 1 Abt Medizinisch-hygienische Bakteriologie, Virusforschung und Parasitologie* 167, 55–64.
- Kane, J.M., Staeger, M.A., Dalton, C.R., Miller, F.P., Dudley, M.W., Ogden, A.M., Kehne, J.H., Ketteler, H.J., McCloskey, T.C., Senyah, Y., *et al.* (1994). 5-Aryl-3-(alkylthio)-4H-1,2,4-triazoles as selective antagonists of strychnine-induced convulsions and potential antispastic agents. *J Med Chem* 37, 125–132.
- Kawamura, A., Graham, J., Mushtaq, A., Tsiftoglou, S.A., Vath, G.M., Hanna, P.E., Wagner, C.R., and Sim, E. (2005). Eukaryotic arylamine N-acetyltransferase. Investigation of substrate specificity by high-throughput screening. *Biochem Pharmacol* 69, 347–359.
- Kawamura, A., Westwood, I., Wakefield, L., Long, H., Zhang, N., Walters, K., Redfield, C., and Sim, E. (2008). Mouse N-acetyltransferase type 2, the homologue of human N-acetyltransferase type 1. *Biochem Pharmacol* 75, 1550–1560.
- Kendall, S.L., Withers, M., Soffair, C.N., Moreland, N.J., Gurcha, S., Sidders, B., Frita, R., Ten Bokum, A., Besra, G.S., Lott, J.S., *et al.* (2007). A highly conserved transcriptional repressor controls a large regulon involved in lipid degradation in *Mycobacterium smegmatis* and *Mycobacterium tuberculosis*. *Mol Microbiol* 65, 684–699.
- Lack, N., Lowe, E.D., Liu, J., Eltis, L.D., Noble, M.E.M., Sim, E., and Westwood, I.M. (2008). Structure of HsaD, a steroid-degrading hydrolase, from *Mycobacterium tuberculosis*. *Acta Crystallogr Sect F Struct Biol Cryst Commun* 64, 2–7.
- Lack, N., Kawamura, A., Fullam, E., Laurieri, N., Beard, S., Russell, A. J., Evangelopoulos, D., Westwood, I., and Sim, E. (2009a). Temperature stability of proteins essential for the intracellular survival of *Mycobacterium tuberculosis*. *Biochemical J* 418, 369–378.
- Lack, N.A., Yam, K.C., Lowe, E.D., Horsman, G.P., Owen, R.L., Sim, E., and Eltis, L.D. (2009b). Characterization of a C-C hydrolase from *Mycobacterium tuberculosis* involved in cholesterol metabolism. *J Biol Chem.* In press. DOI 10.1074/jbc.M109.058081.
- Ley, S.V., Baxendale, I.R., Bream, R.N., Jackson, P.S., Leach, A.G., Longbottom, D.A., Nesi, M., Scott, J.S., Storer, I., and Taylor S.J. (2000). Multi-step organic synthesis using solid-supported reagents and scavengers: a new paradigm in chemical library generation. *J Chem Soc, Perkin Trans 1* 23, 3815–4195.
- Lin, G., Li, D., de Carvalho, L.P., Deng, H., Tao, H., Vogt, G., Wu, K., Schneider, J., Chidawanyika, T., Warren, J.D., *et al.* (2009). Inhibitors selective for mycobacterial versus human proteasomes. *Nature* 461, 621–626.
- Macaev, F., Rusu, G., Pogrebnoi, S., Gudima, A., Stingaci, E., Vlad, L., Shvets, N., Kandemirli, F., Dimoglo, A., and Reynolds, R. (2005). Synthesis of novel 5-aryl-2-thio-1,3,4-oxadiazoles and the

- study of their structure-anti-mycobacterial activities. *Bioorg Med Chem* 13, 4842–4850.
- Makarov, V., Manina, G., Mikusova, K., Mollmann, U., Ryabova, O., Saint-Joanis, B., Dhar, N., Pasca, M.R., Buroni, S., Lucarelli, A.P., *et al.* (2009). Benzothiazinones kill *Mycobacterium tuberculosis* by blocking arabinan synthesis. *Science* 324, 801–804.
- Malbec, F., Milcent, R. and Barbier, G. (1984). Derivatives of 2,4-dihydro-1,2,4-triazole-3-thione and 2-amino-1,3,4-thiadiazole from thiosemicarbazones of esters. *J Heterocycl Chem* 21, 1689–1698.
- Maxmen, A., and Clifton E.B., III (2009). TB's strategic opponent. *J Exp Med* 206, 494–495.
- Moskowitz, H., Mignot, A. and Miocque, M. (1980). On the synthesis of thiazolotriazolylacetic acids. *J Heterocycl Chem* 17, 1321–1323.
- Nagy, J.M., Cass, A.E., and Brown, K.A. (1997). Purification and characterization of recombinant catalase-peroxidase, which confers isoniazid sensitivity in *Mycobacterium tuberculosis*. *J Biol Chem* 272, 31265–31271.
- Neyrolles, O., Hernandez-Pando, R., Pietri-Rouxel, F., Fornes, P., Tailleux, L., Barrios Payan, J.A., Pivert, E., Bordat, Y., Aguilar, D., Prevost, M.C., *et al.* (2006). Is adipose tissue a place for *Mycobacterium tuberculosis* persistence? *PLoS ONE* 1, e43.
- Nodzu, R., Watanabe, H., Kuwata, S., Nagaishi, C., and Teramatsu, T. (1954). Chemotherapy of tuberculosis. IV. Syntheses of m- and p-aminophenol alkyl ethers and their bacteriostatic actions on *Mycobacterium tuberculosis*. *Yakugaku Zasshi* 74, 872–875.
- Pangborn, A.B., Giardello, M.A., Grubbs, R.H., Rosen, R.K., and Timmers, F.J. (1996). Safe and convenient procedure for solvent purification. *Organometallics* 15, 1518–1520.
- Payton, M., Auty, R., Delgoda, R., Everett, M., and Sim, E. (1999). Cloning and characterization of arylamine N-acetyltransferase genes from *Mycobacterium smegmatis* and *Mycobacterium tuberculosis*: increased expression results in isoniazid resistance. *J Bacteriol* 181, 1343–1347.
- Pettersen, E.F., Goddard, T.D., Huang, C.C., Couch, G.S., Greenblatt, D.M., Meng, E.C., and Ferrin, T.E. (2004). UCSF Chimera—a visualization system for exploratory research and analysis. *J Comput Chem* 25, 1605–1612.
- Raman, K., Rajagopalan, P., and Chandra, N. (2005). Flux balance analysis of mycolic acid pathway: targets for anti-tubercular drugs. *PLoS Comput Chem* 1, e46.
- Rengarajan, J., Bloom, B.R., and Rubin, E.J. (2005). Genome-wide requirements for *Mycobacterium tuberculosis* adaptation and survival in macrophages. *Proc Natl Acad Sci U S A* 102, 8327–8332.
- Russell, A.J., Westwood, I.M., Crawford, M.H., Robinson, J., Kawamura, A., Redfield, C., Laurieri, N., Lowe, E.D., Davies, S. G., and Sim, E. (2009). Selective small molecule inhibitors of the potential breast cancer marker, human arylamine N-acetyltransferase 1, and its murine homologue, mouse arylamine N-acetyltransferase 2. *Bioorg Med Chem* 17, 905–918.
- Sali, A., and Blundell, T.L. (1993). Comparative protein modelling by satisfaction of spatial restraints. *J Mol Biol* 234, 779–815.
- Sandy, J., Mushtaq, A., Kawamura, A., Sinclair, J., Sim, E., and Noble, M. (2002). The structure of arylamine N-acetyltransferase from *Mycobacterium smegmatis*—an enzyme which inactivates the anti-tubercular drug, isoniazid. *J Mol Biol* 318, 1071–1083.
- Sikora, A.L., Frankel, B.A., and Blanchard, J.S. (2008). Kinetic and chemical mechanism of arylamine N-acetyltransferase from *Mycobacterium tuberculosis*. *Biochemistry* 47, 10781–10789.
- Sim, E., Sandy, J., Evangelopoulos, D., Fullam, E., Bhakta, S., Westwood, I., Krylova, A., Lack, N., and Noble, M. (2008). Arylamine N-acetyltransferases in mycobacteria. *Current Drug Metabolism* 9, 510–519.
- Sinclair, J.C., Sandy, J., Delgoda, R., Sim, E., and Noble, M.E. (2000). Structure of arylamine N-acetyltransferase reveals a catalytic triad. *Nat Struct Biol* 7, 560–564.
- Singh, R., Fiakpui, C., Galpin, J., Stewart, J., Singh, M.P., and Micetich, R.G. (1996). Synthesis and structure-activity relationship of C-3 substituted triazolythiomethyl cepheems. *Eur J Med Chem* 31, 301–309.
- Stewart, G.R., Newton, S.M., Wilkinson, K.A., Humphreys, I.R., Murphy, H.N., Robertson, B.D., Wilkinson, R.J., and Young, D.B. (2005). The stress-responsive chaperone alpha-crystallin 2 is required for pathogenesis of *Mycobacterium tuberculosis*. *Mol Microbiol* 55, 1127–1137.
- Story, A., van Hest, R., and Hayward, A. (2006). Tuberculosis and social exclusion. *BMJ* 333, 57–58.
- Upton, A.M., Mushtaq, A., Victor, T.C., Sampson, S.L., Sandy, J., Smith, D.M., van Helden, P.V., and Sim, E. (2001). Arylamine N-acetyltransferase of *Mycobacterium tuberculosis* is a polymorphic enzyme and a site of isoniazid metabolism. *Mol Microbiol* 42, 309–317.
- Van der Geize, R., Yam, K., Heuser, T., Wilbrink, M.H., Hara, H., Anderton, M.C., Sim, E., Dijkhuizen, L., Davies, J.E., Mohn, W.W., *et al.* (2007). A gene cluster encoding cholesterol catabolism in a soil actinomycete provides insight into *Mycobacterium tuberculosis* survival in macrophages. *Proc Natl Acad Sci U S A* 104, 1947–1952.
- Verdonk, M.L., Cole, J.C., Hartshorn, M.J., Murray, C.W., and Taylor, R.D. (2003). Improved protein-ligand docking using GOLD. *Proteins* 52, 609–623.
- Wallace, A.C., Laskowski, R.A., and Thornton, J.M. (1995). LIGPLOT: a program to generate schematic diagrams of protein-ligand interactions. *Protein Eng* 8, 127–134.
- Wang, W., Zhang, C., Marimuthu, A., Krupka, H.I., Tabrizizad, M., Shelloe, R., Mehra, U., Eng, K., Nguyen, H., Settachatgul, C., *et al.* (2005). The crystal structures of human steroidogenic factor-1 and liver receptor homologue-1. *Proc Natl Acad Sci U S A* 102, 7505–7510.
- Weber, W.W., and Hein, D.W. (1985). N-acetylation pharmacogenetics. *Pharmacol Rev* 37, 25–79.
- Westwood, I.M., Holton, S.J., Rodrigues-Lima, F., Dupret, J.M., Bhakta, S., Noble, M.E., and Sim, E. (2005). Expression, purification, characterization and structure of *Pseudomonas aeruginosa* arylamine N-acetyltransferase. *Biochem J* 385, 605–612.
- Westwood, I.M., Kawamura, A., Fullam, E., Russell, A.J., Davies, S. G., and Sim, E. (2006). Structure and mechanism of arylamine N-acetyltransferases. *Curr Top Med Chem* 6, 1641–1654.
- Yam, K.C., D'Angelo, I., Kalscheuer, R., Zhu, H., Wang, J.X., Snieckus, V., Ly, L.H., Converse, P.J., Jacobs, W.R., Jr., Strynadka, N., *et al.* (2009). Studies of a ring-cleaving dioxygenase illuminate the role of cholesterol metabolism in the pathogenesis of *Mycobacterium tuberculosis*. *PLoS Pathog* 5, e1000344.